International Journal of Astrobiology 16 (2): 143–155 (2017)
doi:10.1017/S1473550416000203

Study of interaction and adsorption of aromatic amines by manganese oxides and their role in chemical evolution

Brij Bhushan[1], Arunima Nayak[2] and Kamaluddin[3]

[1]*Department of Chemistry, Graphic Era University, Dehradun-248002 (U.K.), India e-mail: brijbhushaniitr@gmail.com*
[2]*IRIS Research-Engineering-Technology, Castelldefels, Barcelona 08860, Spain*
[3]*Department of Chemistry, Indian Institute of Technology Roorkee, Roorkee-247667 (U.K.), India*

Abstract: The role of manganese oxides in concentrating organic moieties and offering catalytic activity for prebiotic reactions is investigated by studying their interaction with different aromatic amines such as aniline, p-chloroaniline, p-toluidine and p-anisidine. For all amines, metal oxides showed highest adsorption at neutral pH. The order of their adsorption capacity and affinity as revealed by the Langmuir constants was found to be manganosite (MnO) > bixbyite (Mn_2O_3) > hausmannite (Mn_3O_4) > and pyrolusite (MnO_2). At alkaline pH, these manganese oxides offered their surfaces for oxidation of amines to form coloured oligomers. Analysis of the oxidation products by gas chromatography–mass spectrometry showed the formation of a dimer from p-anisidine and p-chloroaniline, while a trimer and tetramer is formed from p-toluidine and aniline, respectively. A reaction mechanism is proposed for the formation of the oligomers. While field-emission scanning electron microscopic studies confirm the binding phenomenon, the Fourier transform infrared spectroscopy analysis suggests that the mechanism of binding of amines on the manganese oxides was primarily electrostatic. The adsorption behaviour of the studied aromatic amines followed the order: *p*-anisidine > *p*-toluidine > aniline > *p*-chloroaniline, which is related to the basicities and structure of the amines. Our studies confirmed the significance of the role of manganese oxides in prebiotic chemistry.

Received 11 November 2015, accepted 16 April 2016, first published online 10 May 2016

Key words: adsorption, aromatic amines, manganese oxides, prebiotic chemistry.

Introduction

The basic platform for all the prebiotic reaction producing polymeric substances from which life has emerged is believed to be solid surfaces which are not only abundantly available on Earth's crust, but also have good adsorption and catalytic capacity. Earlier studies have propounded that clay minerals might have concentrated biomolecules and catalysed their oligomerization during the course of chemical evolution (Bernal 1951). Clay and clay minerals have been found to interact with a wide variety of organic molecules such as amino acids, peptides (Greenland *et al*. 1962, 1965; Graf & Laganly 1980), nucleic acid bases (Ferris & Hagan 1986), nucleotides (Furukawa & Brindley 1973; Ferris & Kamaluddin 1979; Ertem & Ferris 1997) and amino acids (Boyd & Mortland 1986; Julian *et al.* 1992; Kowalska *et al.* 2001). The adsorption of organic molecules on clay surfaces took place mainly through cation exchange, ion dipole, coordination and hydrogen bonding. Later studies have highlighted the catalytic activity of metal hexacyanoferrate (II) and its interaction with amino acids (Ali & Kamaluddin 2006), nucleotides (Ali *et al.* 2004a, b; Ali & Kamaluddin 2004, 2007), aromatic amines (Alam *et al.* 2000b, c, 2002; Kamaluddin 2001) and amino pyridines (Viladkar *et al*. 1994; Alam & Kamaluddin 1999, 2000; Alam *et al.* 2000a). It was established that metal hexacyanoferrate (II) was highly efficient in adsorbing amines in neutral as well as alkaline media (pH ~ 9) to bring about oxidation of the amines. Like natural minerals, transition metals may have played a vital role in the chemical evolution by catalysing reactions for formation of biopolymers. Such hypothesis has been amply demonstrated by various studies (Kobayashi & Ponnamperuma 1985a, b; Arora *et al*. 2007; Arora & Kamaluddin 2007, 2009; Uma Shanker *et al.* 2011).

The possible role of manganese oxides in entrapping and aggregating ribose nucleotides has been studied in detail in our earlier studies (Bhushan *et al.* 2011). The results of our study have demonstrated that manganese oxides of lower oxidation state exhibited better adsorptive potential for ribonucleotides and thus may have aided in the catalysis of various reactions necessary for the origin of life. The catalytic activity of manganese for many reactions in the presence of nucleotides, mRNA to give oligoribonucleotides is also reported (Hroacki & Hiromichi 1999). Visscher and Schwartz have concluded that the synthesis of pyrophosphate-linked oligomers from the bis-phosphoimidazolides of deoxyadenosine and deoxyguanosine, as well as from acyclic analogues of these nucleosides, is catalysed much more effectively by Mn (II) (Visscher & Schwartz 1989). In our attempt to further elucidate the role of manganese oxides in the course of chemical evolution, the

present study is to determine its binding potential with different aromatic amines. The basis of selection of aromatic amines in this study is that amines are one of the important classes of organic compounds, which are widely distributed in nature in the form of amino acids, alkaloids and vitamins. The presence of amino acids containing aromatic ring on the primitive Earth has been proposed by Friedmann & Miller (1969). One could, thus reasonably postulate the presence of aromatic amines on the primitive Earth environment.

Experimental and procedure

Material and methods

Manganese acetate (Merck), ammonium oxalate (Merck), aniline, p-anisidine, p-toluidine, p-chloroaniline, acetate, Borax buffer, diphenyl polysiloxane and dimethyl polysiloxane were purchased from Sigma. All other chemicals used were of an analytical grade and were used without further purification. Millipore water was used throughout the studies.

Synthesis and characterization of manganese oxides

Manganese oxides of different Mn/O ratio (manganosite (MnO), hausmannite (Mn_3O_4), bixbyite (Mn_2O_3) and pyrolusite (MnO_2)) were synthesized as described in our earlier works (Bhushan *et al.* 2011). Characterization studies with respect to X-ray diffraction (XRD) revealed the purity of the prepared oxides after comparison with JCPDS XRD patters. The surface area of the oxides were determined by nitrogen (N) adsorption isotherms on micromeritics ASAP 2010 (UK). All manganese oxides had a more or less equal surface area. Details are described in (Bhushan *et al.* 2011).

Adsorption of aromatic amines on manganese oxides

Evaluation of parameters necessary for investigating the adsorption equilibrium

The optimum conditions which were studied for investigating the adsorption equilibrium for the amine and metal oxides were

I. Concentration of adsorbate
II. Particle size of adsorbent
III. Equilibrium time for adsorbate and adsorbent
IV. Quantity of adsorbent
V. Effect of pH and effect of temperature

For determining the adsorption isotherm of amines on manganese oxides a moderate concentration range of amines (2×10^{-5}–1.4×10^{-4} M) were chosen in order to get absorbance of amines in the suitable range of the absorbance scale on the spectrophotometer.

Manganese oxides of various particle sizes were tested and it was found that particle size of 80–100 mesh was the most suitable one. In order to fix up the equilibrium time and quantity of adsorbent for optimum adsorption, experiments were performed varying the time of contact (30 min to 24 h) and the amount of metal oxides at a fixed adsorbate concentration (5×10^{-4} M). It was observed that the maximum adsorption took place when the amount used was 50 mg/10 ml of adsorbent solution for aniline, p-toluidine, p-anisidine and p-chloroaniline for 24 h. Adsorption of p-chloroaniline on a metal oxide was found to be a slow process and equilibrium was found to establish after 72 h.

Adsorption of amine was studied over wide pH range (4–9) on all metal oxides. Buffer used to maintain pH were acetate (pH 4–7) and Borax (pH ~ 9). It was found that adsorption of aromatic amines on manganese oxide was negligible in acidic and basic media. A neutral pH range (6.8–7.12) was found to be suitable for maximum adsorption.

Fourier transform infrared spectroscopy (FTIR) analysis

In order to elucidate the mechanism of binding or interaction of amines onto the oxides, IR spectra of adsorbates, adsorbent, and adsorption adducts were recorded on a Perkin-Elmer 1600 FTIR spectrophotometer using KBr pellets.

Batch adsorption experiments

Preliminary experiments were initially carried out to find out the suitable conditions for the maximum adsorption of amines. A series of 50 ml glass test tubes were employed and each tube was filled with 10 ml of amine solution of varying concentration (2.0×10^{-5}–1.4×10^{-4} M). MnO, Mn_2O_3, Mn_3O_4 and MnO_2 (100 mg) was added to each tube. The pH of the solution was adjusted to the desired value using acetate or borax buffers. Species of these buffers did not get adsorbed onto the manganese oxide surface. This was verified by conductivity measurements as there was no change in the inflection point of buffers with and without manganese oxides. The tubes were shaken with a Spinix vortex shaker initially for 1 h and then allowed it to equilibrate at 25°C with intermittent shaking at fixed time intervals. The equilibrium was attained within 6 h. The equilibrium time and concentration range were, however, decided after a good deal of preliminary investigations. The amount of amine adsorbed was calculated as the difference between amine concentration before and after adsorption. The concentration of amine at equilibrium and the amount adsorbed were used to obtain the adsorption isotherm.

Estimation of amines concentrations

The concentration of aromatic amines was estimated spectrophotometrically which involved the measurement of amine at the wavelength of maximum absorption (λ_{max}). Electronic spectra of ribose nucleotides were recorded using Shimadzu UV–1601 spectrophotometer (Model UV-188-240V, Shimadzu Corporation Kyoto, Japan) which showed characteristic λ_{max} values of amines at 280, 295, 290 and 286 nm, for aromatic amines namely aniline, p-anisidine, p-chloroaniline and p-toluidine, respectively.

Determination of adsorption isotherms

The equilibrium concentration of adsorbate (C_{eq}) and the amount (X_e) adsorbed per gram adsorbent was used to study the adsorption isotherms.

https://doi.org/10.1017/S1473550416000203 Published online by Cambridge University Press

The amount of adsorbate which adsorbed on 1 g of adsorbent (X_e) was calculated using the formula:

$$X_e = \frac{(C_i - C_{eq}) \times v \times M \times 1000}{w},$$

where X_e, Amount (mg) of adsorbate adsorbed on 1 g of adsorbent; C_i, Initial concentration of adsorbate (mole/l); C_{eq}, equilibrium concentration of adsorbate (mole/l); V, volume of adsorbate solution (l); M, molecular weight of adsorbate; and w, amount (mg) of adsorbent used.

Determination of per cent binding

The per cent binding of aromatic amines on metal oxides under study was determined at the saturation point of adsorption isotherms. The per cent binding was calculated from the concentration of adsorbate before and after adsorption as shown below:

$$\%\text{Binding} = \left(\frac{\text{Concentration of adsorbate before adsorption} - \text{Concentration of adsorbate after adsorption}}{\text{Concentration of adsorbate before adsorption}} \right) \times 100$$

Analysis of oxidation reaction products by gas chromatography–mass spectrometry (GC–MS)

In alkaline medium (pH > 8) brown-red coloured products of oxidized amine were deposited on the manganese oxides (MnO, Mn_2O_3, Mn_3O_4 and MnO_2) surfaces within 24 h. These coloured products were extracted and concentrated in benzene for GC–MS analysis. Products thus formed were analysed on a GC–MS (Perkin Elmer–Claurus-500) with FID detector equipped with a capillary column (ELITE-1 with stationary phase 100% dimethyl polysiloxane column length 30 m, diameter 0.32 mm). The conditions for GC were as follows: Injector temperature, 250°C; transfer line temperature, 250°C. The capillary column temperature was programmed as follows: 80°C for 2 min; from 80 to 260°C at 10°C min^{-1}, held at 250°C for 15 min. Helium was used as a carrier gas with a flow rate of 2 ml min^{-1}. The mass spectrometer conditions were ion source 250°C and ionization energy 40 eV.

Results

Adsorption isotherms of aniline, p-chloroaniline, p-toluidine and p-anisidine in the present case show that irrespective of the adsorbent (manganese oxides), the isotherms are regular, positive and concave to the concentration axis (Figs. 1–4). The initial portion of the isotherms shows a linear relationship between the amount adsorbed and equilibrium concentration showing that the adsorption is very fast initially. At the higher concentration range, saturation phenomenon was observed. Adsorption data were fitted into Langmuir adsorption isotherm (Atkins & DePaul 2002) which assumes the formation of a monolayer of solute molecules on the surface of the

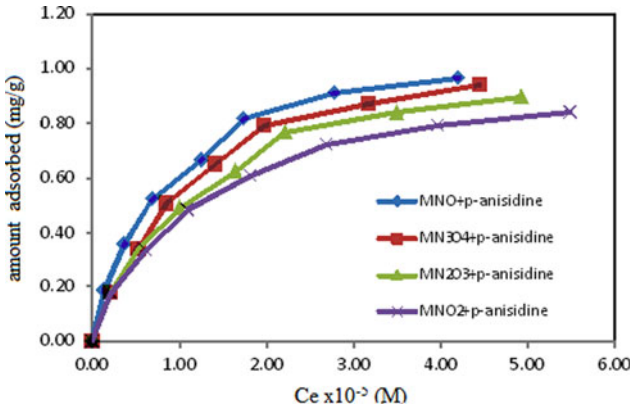

Fig. 1. Adsorption isotherm of p-anisidine on manganese oxides.

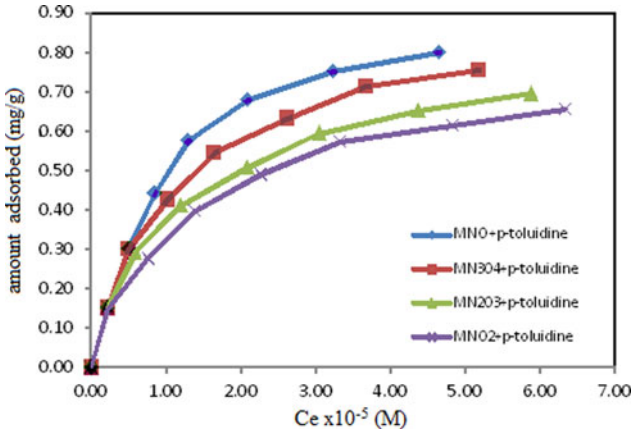

Fig. 2. Adsorption isotherm of p-toluidine on manganese oxides.

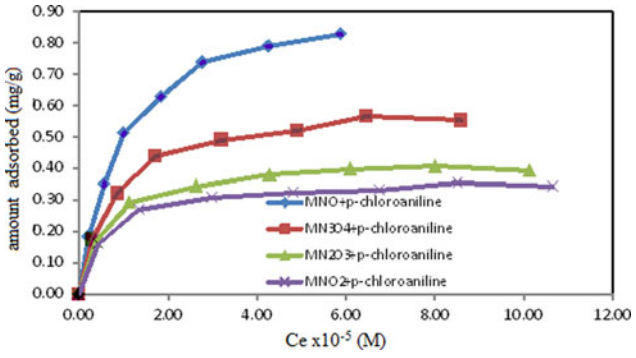

Fig. 3. Adsorption isotherm of p-chloroaniline on manganese oxides.

adsorbent and given by

$$\frac{C_{eq}}{X_e} = \frac{C_{eq}}{X_m} + \frac{1}{X_m} k_L,$$

where C_{eq} is the equilibrium concentration of solute (mole/l); X_e, amount of solute adsorbed per gram weight of adsorbent (mg); X_m, the moles of amines/g of manganese oxide adsorbed at saturation; k_L, Langmuir adsorption constant (litre/mg).

A typical graph of C_{eq}/X_e versus C_{eq} is a straight line represented in Figs. 5–8. X_m and k_L values were calculated from the graphs and tabulated in Table 1. X_m value indicates the maximum amount of amines adsorbed on manganese oxides for

https://doi.org/10.1017/S1473550416000203 Published online by Cambridge University Press

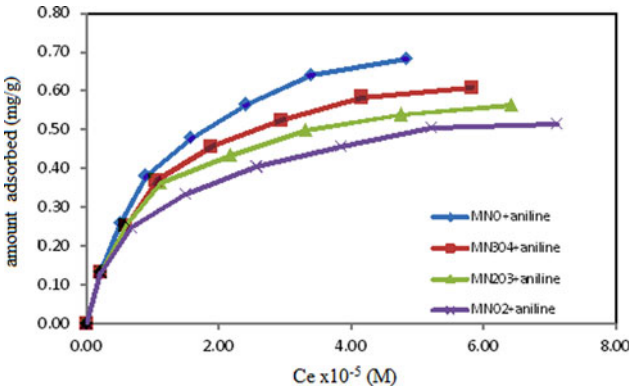

Fig. 4. Adsorption isotherm of aniline on manganese oxides.

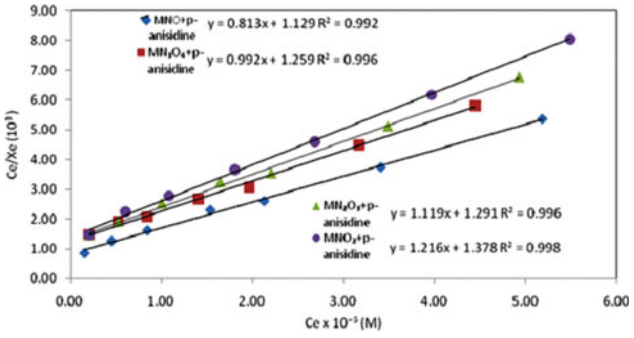

Fig. 5. Langmuir isotherms of p-anisidine on manganese oxides.

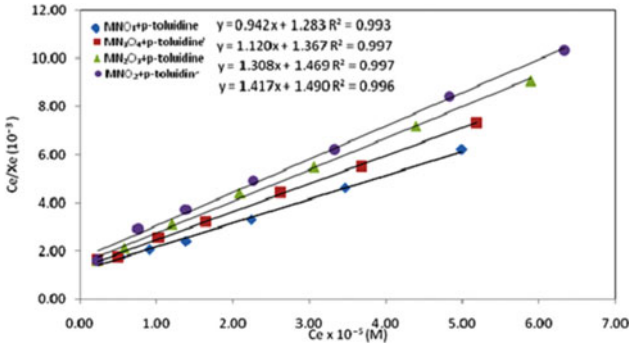

Fig. 6. Langmuir isotherms of p-toluidine on manganese oxides.

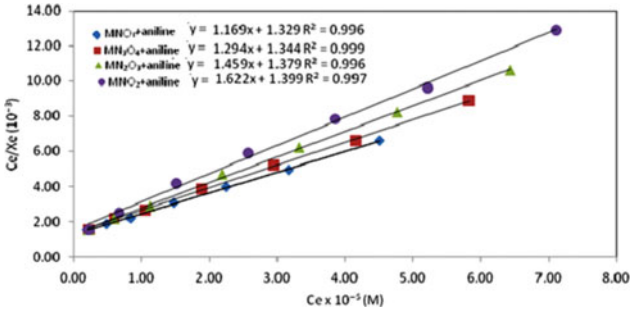

Fig. 7. Langmuir isotherms of aniline on manganese oxides.

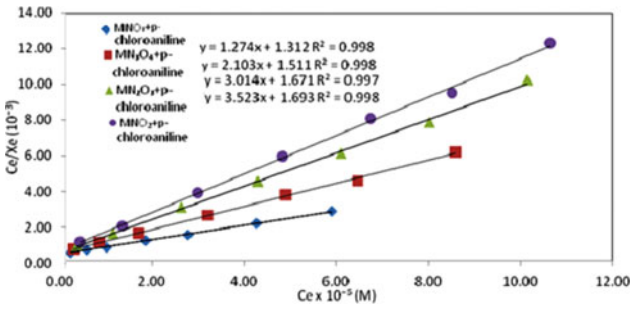

Fig. 8. Langmuir isotherms of p-chloroaniline on manganese oxides.

monolayer formation; k_L value is related to the enthalpy of adsorption (Atkins & de Paul 2002).

The per cent binding of p-anisidine, p-chloroaniline, p-toluidine and aniline, calculated from the adsorption isotherms, is represented in Table 2. In order to determine the nature of binding interaction between the amines and the manganese oxides, the infrared spectra (FTIR) of all manganese oxides before and after adsorption with the studied amines were recorded and analysed. Figures 9–12 indicate the FTIR spectra of MnO, the studied amine and the MnO–amine adduct after adsorption. Other manganese oxides showed similar spectra after adsorption to the studied amines as compared with that of MnO; hence, their spectra were not shown. Field emission scanning electron microscopic (FE-SEM) studies of the amine and manganese oxide were also performed to study the morphological changes on the surface of the manganese oxides after adsorption. The surface of the MnO, Mn_2O_3, Mn_3O_4 and MnO_2 after binding with the studied amines showed similar morphological changes indicating the occurrence of binding. The FE-SEM figures corresponding to MnO, p-anisidine and p-anisidine–MnO adduct (Fig. 13) were only shown.

Further it was also observed that in alkaline medium (pH > 8) all the manganese oxides gave coloured polymerized products with the studied amines. The coloured products from all manganese oxides were individually separated and were identified to be similar. Irrespective of the manganese oxides, a dimer was obtained from both p-chloro-aniline and p-anisidine. A trimer and a tetramer were obtained from p-toluidine and aniline, respectively. The analysis of the polymerized products obtained from MnO has been shown and discussed in the forthcoming sections.

Analysis of oxidation products of aniline with MnO

Mass spectra of the reaction products corresponding to peaks at retention time (R_t) 3.31, 7.29, 16.62 and 25.51 min are shown in Figs. 14–16. Peak with retention time (R_t) 3.31 correspond to that of aniline. The formation of benzoquinone (R_t = 7.29 min) is clearly evidenced by the peaks corresponding to *m*/*z* 108, 82 and 54, in accordance with its fragmentation pattern determined by electron bombardment. However, GC–MS study of the peak with R_t 16.62 min showed the formation of azobenzene confirmed by a peak at *m*/*z* 182. Some other mass peaks in the fragmentation pattern of the product at *m*/*z* 105, 77 and 51

https://doi.org/10.1017/S1473550416000203 Published online by Cambridge University Press

Table 1. *Langmuir constants for adsorption of amines on manganese oxide*

	Manganosite (MnO)		Hausmannite (Mn_3O_4)		Bixbyite (Mn_2O_3)		Pyrolusite (MnO_2)	
Aromatic amine	k_L (litre mg^{-1})	X_m (mg g^{-1})	k_L (litre mg^{-1})	X_m (mg g^{-1})	k_L (litre mg^{-1})	X_m (mg g^{-1})	k_L (litre mg^{-1})	X_m (mg g^{-1})
p-Anisidine	1.39	1.23	1.27	1.01	1.15	0.89	1.13	0.82
p-Toluidine	1.36	1.06	1.22	0.89	1.12	0.76	1.05	0.71
Aniline	1.14	0.86	1.04	0.77	0.95	0.69	0.86	0.62
p-Chloroaniline	1.03	0.78	0.72	0.48	0.55	0.33	0.48	0.28

Table 2. *Per cent binding of amines on manganese oxides*

Aromatic amine	Manganosite (MnO)	Hausmannite (Mn_3O_4)	Bixbyite (Mn_2O_3)	Pyrolusite (MnO_2)
p-Anisidine	81.15	78.69	76.23	71.31
p-Toluidine	75.83	73.33	69.17	67.50
Aniline	73.24	69.72	64.79	61.27
p-Chloroaniline	71.13	50.00	38.03	31.69

were also observed. R_t 25.51 peak corresponds to tetramer of aniline, confirmed by their fragmentation pattern. A well-known mechanism is proposed for the formation of benzoquinone, tetramer of aniline and azobenzene (Figs. 17 and 18).

Analysis of oxidation products of p-anisidine with MnO

In the case of anisidine the chromatogram showed two major peaks with R_t 3.81 and 15.72 min corresponding to anisidine and its dimer, respectively. Mass analysis of the product with R_t 15.72 min showed major peaks at *m/z* 242, 135, and 107 which correspond to fragmentation of anisidine dimer (Fig. 19). A possible mechanism for the formation of dimer of p-anisidine may be proposed as shown in Fig. 20.

Analysis of oxidation products of p-chloroaniline with MnO

In the case of p-chloroaniline the chromatogram showed two major peaks with R_t 3.87 and 30.72 min. Peak with retention time (R_t) 3.87, corresponding to p-chloroaniline, whereas the second peak at retention time (R_t) 30.72 min corresponds to its dimer. Mass analysis of the product with R_t 30.72 min showed major peaks at *m/z* 139, 111, 92 and 77, which correspond to fragmentation of p-chloroaniline dimer (Fig. 21). A possible mechanism for the formation of dimer of p-chloroaniline may be proposed as shown in Fig. 22.

Analysis of oxidation products of p-toluidine with MnO

The oxidation products of p-toluidine gave well defined and well separated peaks in gas chromatogram with R_t 3.25 and 27.59 min. Mass spectra of the peak with R_t 27.59 min showed molar mass 317 (100%), which corresponds to trimer of p-toluidine (Fig. 23). Some high fragments observed were 300, 226, 211, 107, 91 and 77. The above obtained fragmentation mass patterns resembled with the possible fragmentation pattern of a trimer. Peak with R_t 3.25 min corresponds to the starting material, i.e. p-toluidine. Possible mechanism for the formation of dimer of p-toluidine was also proposed (Fig. 24).

Discussion

A neutral pH range (~7.0) was selected for preliminary adsorption studies of aromatic amines on manganese oxides (MnO, Mn_2O_3, Mn_3O_4 and MnO_2). Subsequent studies were performed at pH ~ 7.0 which was optimum for the maximum adsorption of all the amines. The neutral pH is physiologically significant as most of the reactions in living systems take place in neutral media. X_m values also indicate that anisidine adsorption is more in comparison to that of other amines.

Although all manganese oxides had nanosized particles (evidenced from Transmission Electron Microscopy (TEM) studies) and more or less equal surface area (Brunauer–Emmett–Teller (BET) studies) as documented in previous studies (Bhushan *et al.* 2011), yet adsorption results (as indicated by the X_m values in Table 1) reveal that among all manganese oxides, MnO showed the highest binding capacity for all studied amines. The k_L values also indicate highest binding affinity of MnO for the amines. MnO also showed highest binding for ribonucleotides as revealed in our earlier studies (Bhushan *et al.* 2011). In the present study, Table 1 also reveals that all manganese oxides showed a similar trend of binding towards the aromatic amines. Among the studied aromatic amines, irrespective of the manganese oxides, the following adsorptive trend (X_m values) was observed: p-anisidine > p-toluidine > aniline > p-chloroaniline. This observed trend can be best explained by taking into consideration both the aromatic amine solution chemistry and their structure (Chien-To & Hsisheng 2000). A direct correlation was observed between the binding trend of the amines and their basicity in aqueous medium. The basicity or pK_a values of the p-anisidine, p-toluidine, aniline, p-chloroaniline are 5.34, 5.04, 4.63 and 4.15, respectively. While considering the correlation between the structure of the aromatic amines and their binding affinity onto the manganese oxides, it appears that the presence of electron-donating groups on the ring (–OCH_3 of p-anisidine, –CH_3 of p-toluidine) led to a higher binding affinity, while electron-withdrawing groups (–Cl of p-Cl–aniline) resulted in lower affinity onto the manganese oxides. A glance at the possible interactions between the amine–manganese oxides will help in understanding the observed adsorptive trend. Since the adsorption experiments of this work were performed at neutral pH well below the P_{PZC} of the manganese oxides (P_{ZPC} (zero point charge) of MnO, Mn_2O_3, Mn_3O_4 and MnO_2 are >10, >10, 7.7 and 7.3, respectively (Bhushan *et al.* 2011), the surface charge of the manganese oxides was predominantly positive. Taking also into account the pK_a values of the amines, it is expected that at the neutral pH, the amines are in molecular form.

https://doi.org/10.1017/S1473550416000203 Published online by Cambridge University Press

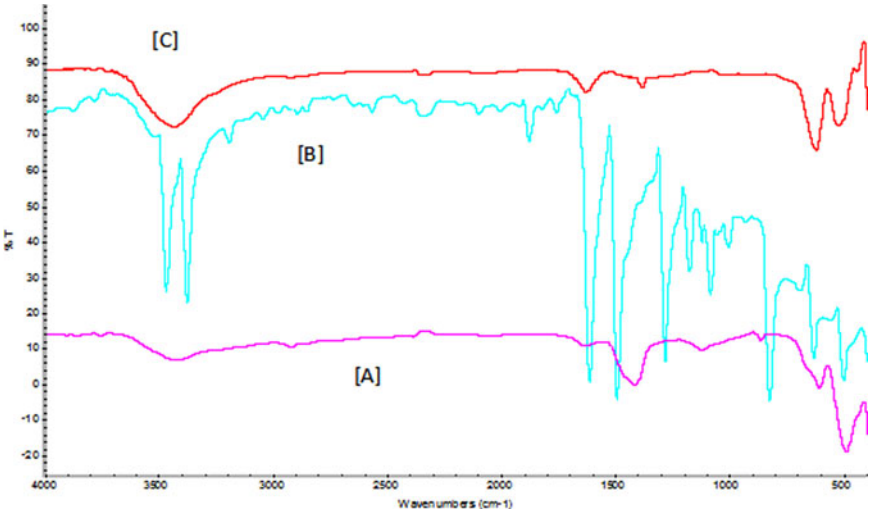

Fig. 9. IR spectra of MnO (A), p-anisidine (B) and p-anisidine–MnO adduct (C).

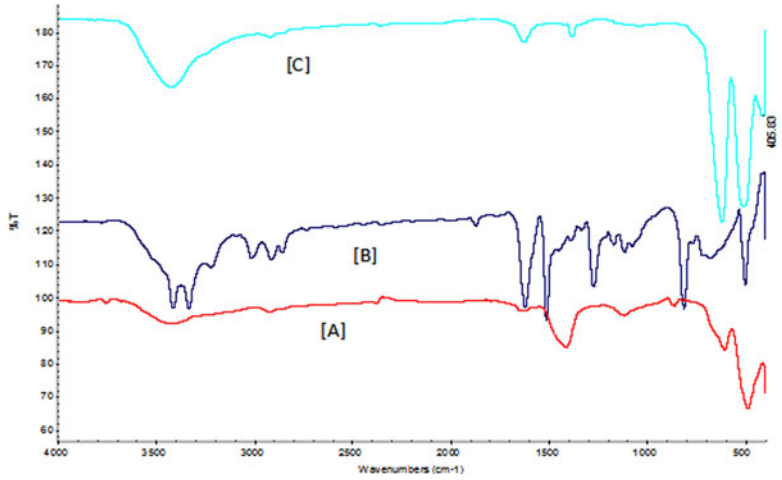

Fig. 10. IR spectra of MnO (A), p-toluidine (B) and p-toluidine-MnO adduct (C).

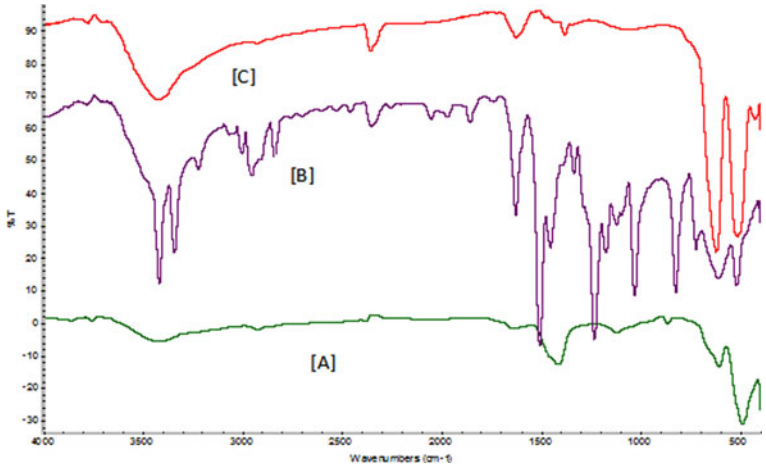

Fig. 11. IR spectra of MnO (A), p-chloroaniline (B) and p-chloroaniline–MnO adduct (C).

Electrostatic interaction between the amines and the manganese oxides was elucidated and confirmed by means of infrared absorption (FTIR) study. FTIR spectra (Figs. 9–12) reveals the presence of additional and prominent peaks at frequencies 1560 cm^{-1} (corresponding to NH bend of amines) and at 1350 cm^{-1} (corresponding to CN stretch) on all MnO–amine

https://doi.org/10.1017/S1473550416000203 Published online by Cambridge University Press

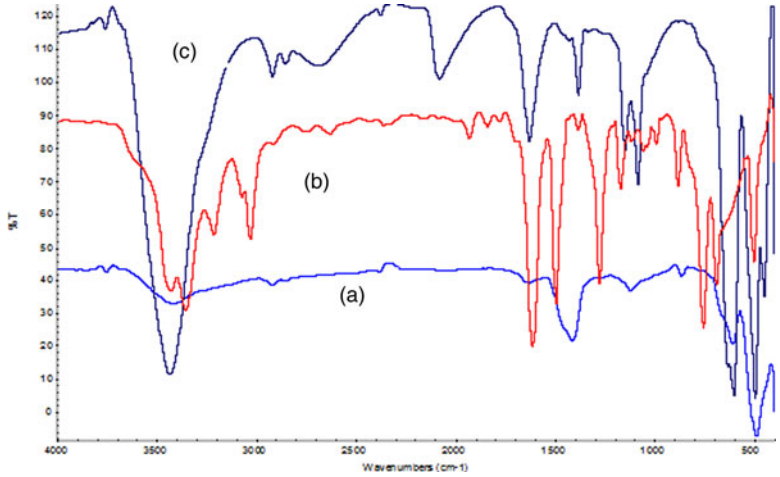

Fig. 12. IR spectra of MnO (A), aniline (B) and aniline–MnO adduct (C).

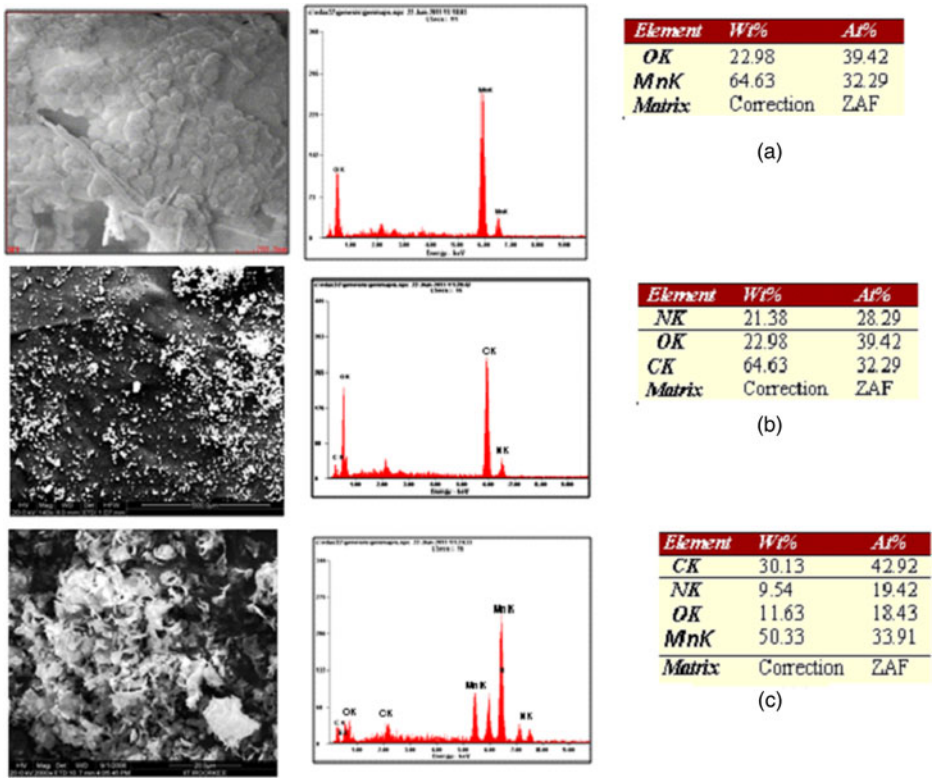

Fig. 13. FE-SEM photographs of MnO (A), p-anisidine (B) and MnO–p-anisidine adduct (C).

adducts. This reveals that the protonated manganese oxides were bound to the neutral amines via their amine functionality. Since similar observations were made from the FTIR spectra of Mn_2O_3, Mn_3O_4 and MnO_2–amine adducts; the figures were hence not shown. Thus electrostatic interactions between the positively charged surface of manganese oxides (MnO and other manganese oxides) with the amines may have taken place through the lone pair of electrons on the N atom and also probably via the π electrons of the aromatic ring (Yao & Millero 1996). Similar observations were made by Alam *et al.* (2000b) and Shankar *et al.* (2013) while studying the binding interaction of aromatic amines with metal hexacyanoferrate and iron oxides. Electrostatic interaction was also postulated as the major binding mechanism by Daou *et al.* (2007) and on magnetite and goethite (Li & Stanforth 2000; Antelo *et al.* 2005; Chitrakar *et al.* 2006).

The evidence of binding of the amines onto the manganese oxides is further evident from FE-SEM images. Figures 13(c) corresponding to the surface of amine–MnO adduct reveals significant morphological changes as compared with Fig. 13 (a) which corresponds to that of MnO surface. Similar observations were seen on the surface of other manganese oxide–amine adducts; hence the figures were not shown. Energy-dispersive X-ray (EDX) pattern of Fig. 13(c) shows a distinct increase

https://doi.org/10.1017/S1473550416000203 Published online by Cambridge University Press

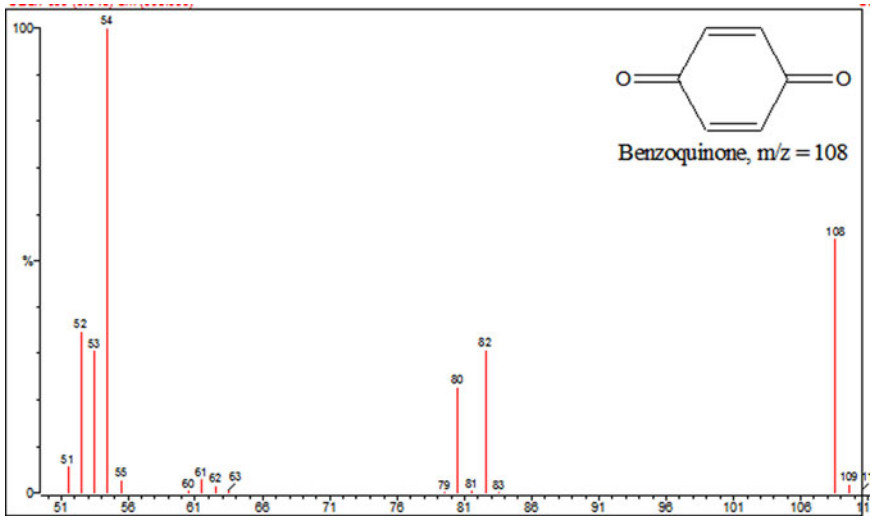

Fig. 14. Mass spectrum of benzoquinone.

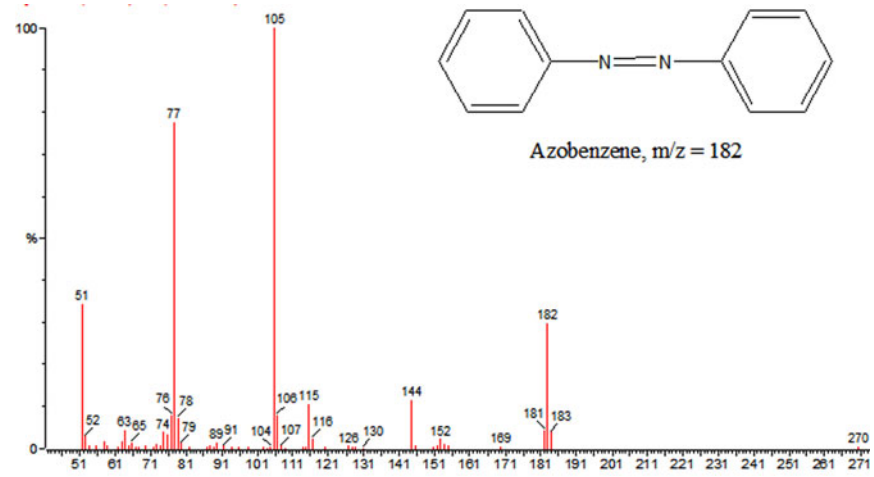

Fig. 15. Mass spectrum of azobenzene.

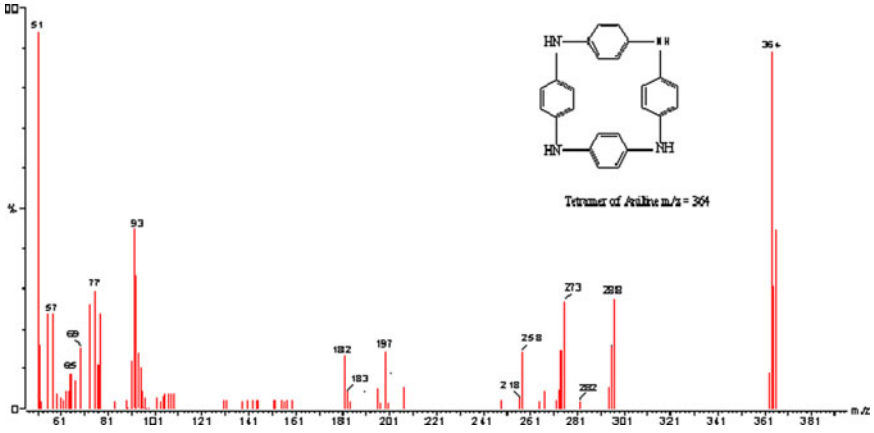

Fig. 16. Mass spectrum of tetramer of aniline.

in percentage of N and carbon from that of Fig. 13(a). Similar finding in the EDX pattern of other manganese oxides were observed thereby supporting the binding of amines onto the manganese oxides.

While studying the interaction of the amines with the manganese oxides, it was observed that coloured products were obtained. Such products were identified by mass spectra results to be oligomers. The oligomers formed were similar irrespective

https://doi.org/10.1017/S1473550416000203 Published online by Cambridge University Press

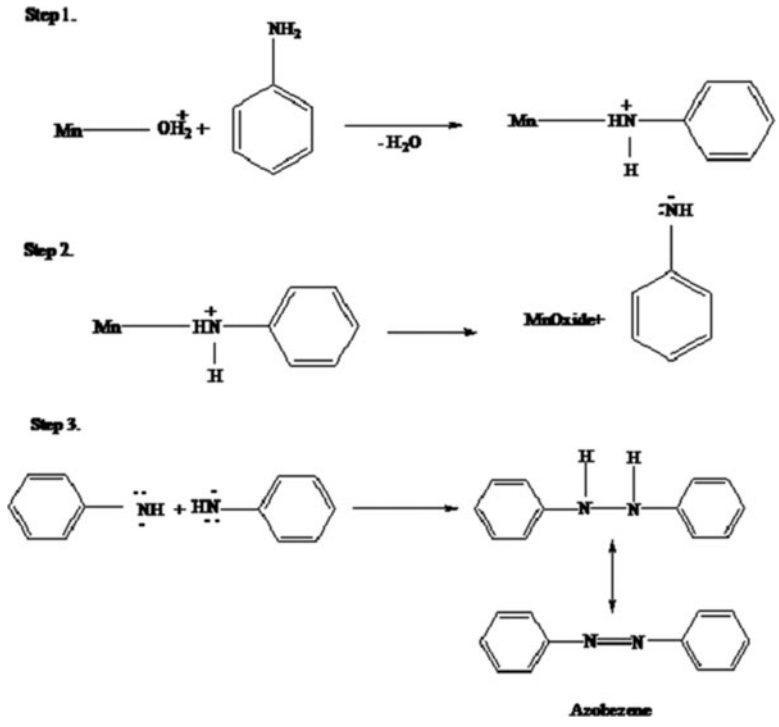

Fig. 17. Proposed mechanism for the formation of azobenzene.

of the manganese oxides. This reveals that the manganese oxides played a catalytic role in the polymerization reactions. While the oxidation products were identified as dimers from p-anisidine and p-chloroaniline, trimers and tetramers were identified from p-toluidine and aniline, respectively. Aromatic compounds have earlier demonstrated oligomerization or polymerization reactions on clay surfaces (Issacson & Sawhney 1983; Boyd & Mortland 1986; Govindraj *et al.* 1987; Soma & Soma 1989; Kowalska & Cocke 1992), on metal hexacyanoferrates (Alam *et al.* 2000c) and on the surface of iron oxides (Shanker *et al.* 2013). It is reasonable hence to assume similar interactions and reaction products occurred between the aromatic amines and manganese oxides.

On the basis of the mass spectra studies carried out on the reaction products, the most probable structure and tentative mechanism are proposed (Figs. 17 and 18 for aniline oligomers, Fig. 20 for p-anisidine dimers, Fig. 22 for p-chloro-aniline dimers and Fig. 24 for p-toluidine trimer). The oxidation and polymerization reaction might have occurred as follows as proposed by Laha & Luthy (1990); Pizzigallo *et al.* (1998). In a manganese oxide/water system, the surface of the oxide can be represented as Mn oxide-OH_2^+ or Mn-OH depending on the pH of the aqueous medium and the P_{ZPC} of the oxide. In the first step, a protonated surface complex is formed by interaction of the aniline molecule and the manganese oxide. Another aniline molecule is involved in the interaction whereby an anilino molecule is liberated. The manganese in the complex is simultaneously reduced. The surface complex then releases the reduced manganese and a second anilino molecule is liberated. The anilino molecules released from the surface complex are stabilized by resonance with the lone electrons localized on the N atom or at the ortho and para positions, it can enter into oxidative coupling reactions. Dimers can be formed either by N–N, N-ortho or N-para radical couplings. The predominance of a dimer depends on the extent of localization of lone electrons in the N, ortho or para positions. The N–N coupling gives rise to 4,4′ hydrazobenzene which undergoes further oxidation to 4,4′ azobenzene. The N-para coupling gives rise to four aminophenyl analine which undergoes further oxidation to benzoquinone. This coupling phenomenon continues to give rise to a trimer or a tetramer.

Manganese oxides with different oxidation states like 2, 3 and 4 exist (Burns *et al.* 1985; Bish & Post 1988; Shen *et al.* 1992; De Guzman *et al.* 1993) with decreasing average volume per Mn ion (A3) in each form of the oxide (Li & Stanforth 2000). Since the prebiotic condition existing in the bottom of sea was essentially reducing (Oparin 1938; Urey 1952; Miller 1953), the possibility of existence of manganese oxide in its reduced state (MnO) would have been more probable in the early life conditions. But with increasingly change of the primitive Earth's atmosphere to more oxidizing nature (Jortner 2006). Thus under such conditions, the adsorption which is the first step to origin of life would have occurred on MnO. Similar findings were made in our earlier study which proved that MnO offered highest binding affinity to nucleotides.

Conclusion

The present research has proved the hypothesis that manganese oxides might have been involved in early stages of chemical evolution of life. The implications of this research in prebiotic chemistry are of significance because it has shown experimentally that manganese oxide having lower metal oxygen ratio have provided good adsorption sites for concentrating

https://doi.org/10.1017/S1473550416000203 Published online by Cambridge University Press

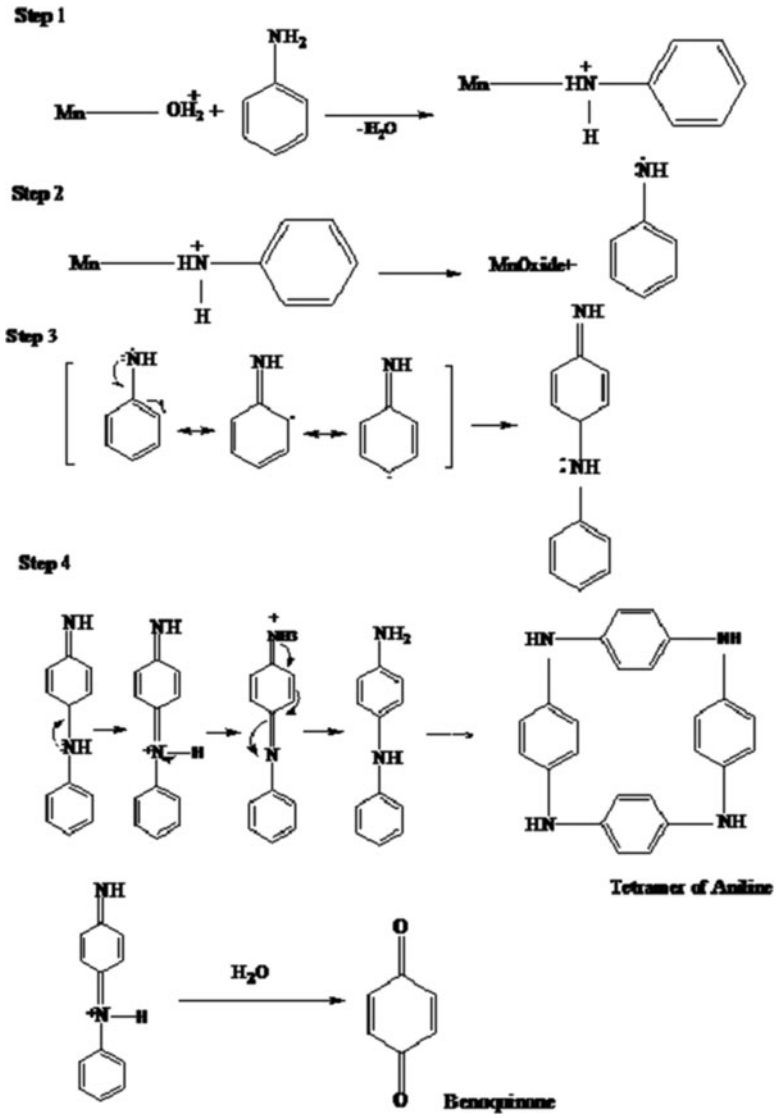

Fig. 18. Proposed mechanism for the formation of tetramer of aniline and benzoquinone.

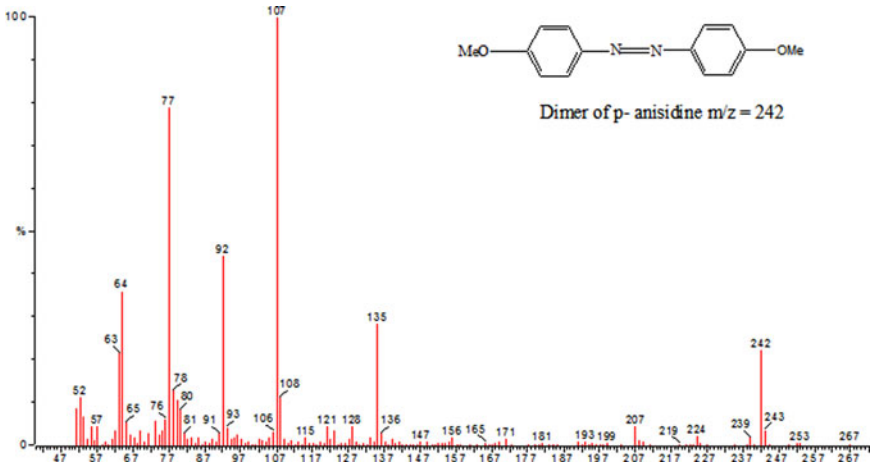

Fig. 19. Mass spectrum of dimer of p-anisidine.

https://doi.org/10.1017/S1473550416000203 Published online by Cambridge University Press

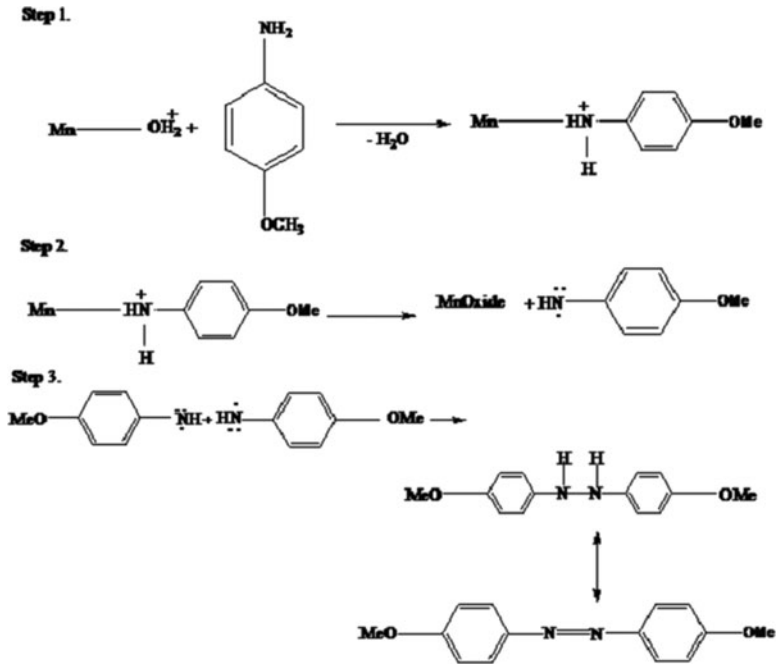

Fig. 20. Proposed mechanism for the formation of dimer of p-anisidine.

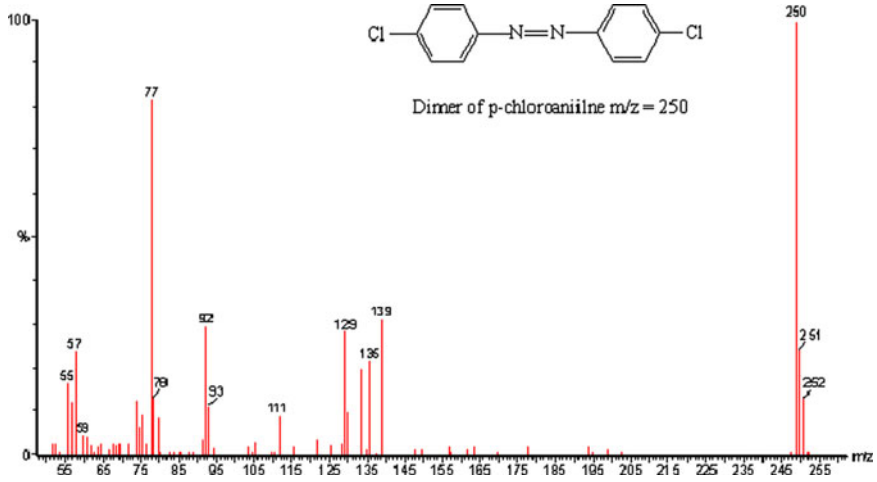

Fig. 21. Mass spectrum of dimer of p-chloroaniline.

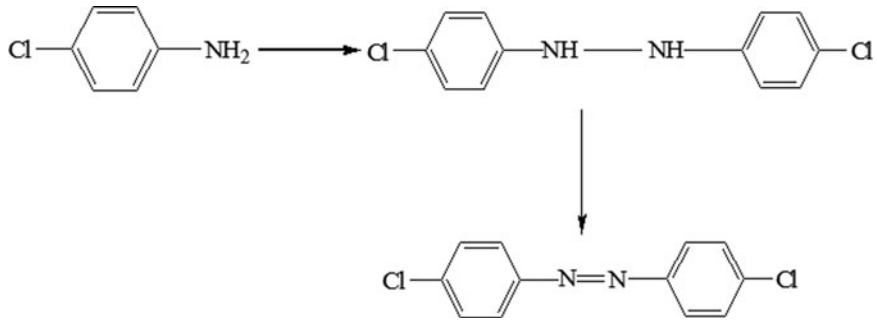

Fig. 22. Proposed mechanism for the formation of dimer of p-chloroaniline.

https://doi.org/10.1017/S1473550416000203 Published online by Cambridge University Press

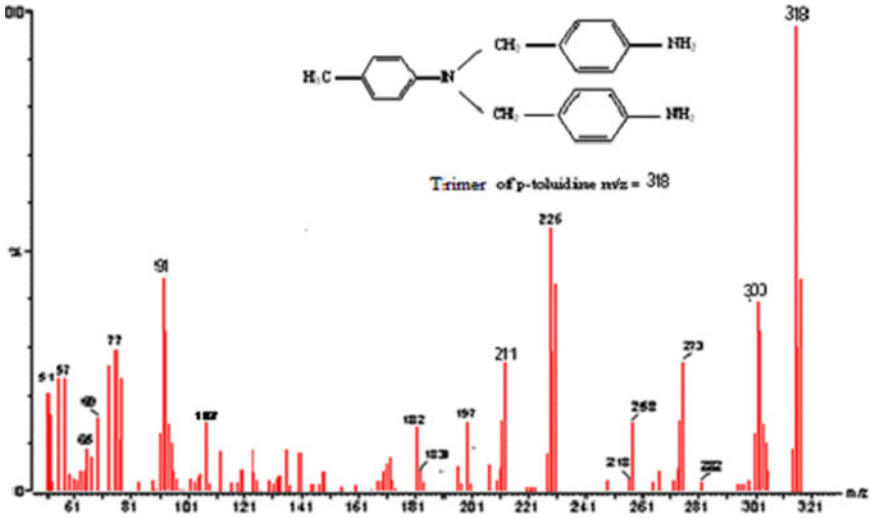

Fig. 23. Mass spectrum of trimer of p-toluidine.

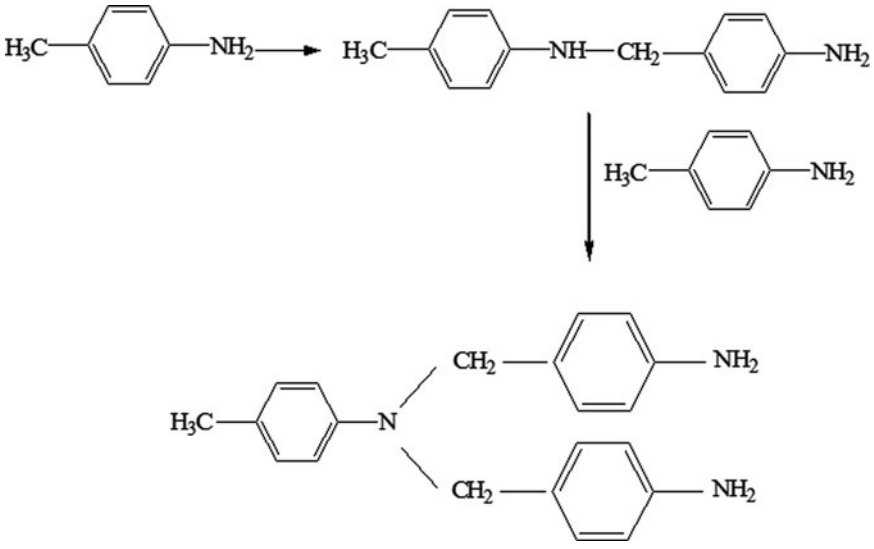

Fig. 24. Proposed mechanism for the formation of trimer of p-toluidine.

important organic molecules like aromatic amines and have also helped in catalysing the subsequent polymerization reactions.

Acknowledgement

We are grateful to Indian Space Research Organization (ISRO), Bangalore, India, for financial support.

References

Alam, T. & Kamaluddin (1999). *Bull. Chem. Soc. Jpn*. **72**, 1697–1703.
Alam, T. & Kamaluddin (2000). *Colloids Surf*. **162**, 89–97.
Ali, S. & Kamaluddin (2004). *Bull. Chem. Soc. Jpn*. **77**, 1681–1686.
Ali, S. & Kamaluddin (2006). *Bull. Chem. Soc. Jpn*. **79**, 1541–1546.
Ali, S. & Kamaluddin (2007). *Orig. Life. Evol. Biosph*. **37**, 225–234.
Alam, T., Tarannum, H., Kumar, N. & Kamaluddin (2000a). *J. Colloid Interface Sci*. **224**, 133–139.
Alam, T., Tarannum, H., Ravi, M.N.V. & Kamaluddin (2000b). *Talanta* **51**, 1097–1105.
Alam, T., Gairola, P., Tarannum, H., Kamaluddin & Ravi, M.N.V. (2000c). *Indian J. Chem. Technol*. **7**, 230–235.
Alam, T., Tarannum, H., Ali, S. & Kamaluddin (2002). *J. Colloid Interface Sci*. **245**, 251–256.
Ali, S., Ahmad, J. & Kamaluddin (2004a). *Colloids Surf. A: Physicochem. Eng. Aspects* **236**, 165–169.
Ali, S., Alam, T. & Kamaluddin (2004b). *Astrobiology* **4**, 420–426.
Antelo, J., Avena, M., Fiol, S., Lopez, R. & Arce, F. (2005). *J. Colloid Interface Sci*. **285**, 476–486.
Arora, A.K. & Kamaluddin (2007). *Colloids Surf. A: Physicochem. Eng. Aspect* **298**, 186–191.
Arora, A.K. & Kamaluddin (2009). *Astrobiology* **9**, 165–171.
Arora, A.K., Tomar, V., Aarti, N., Venkateswararao, K. T. & Kamaluddin (2007). *Int. J. Astrobiol*. **6**, 267–271.
Atkins, P. & de Paul, J. (2002). *Atkins' Physical Chemistry*, 7th edn. Oxford University Press, Oxford.
Bernal, J.D. (1951). *The Physical Basis of Life*. Routledge and Kegan Paul, London, p. 34.
Bish, D.L. & Post, J.E. (1988). *Am. Mineral*. **74**, 861–869.

https://doi.org/10.1017/S1473550416000203 Published online by Cambridge University Press

Bhushan, B., Shanker, U. & Kamaluddin (2011). *Orig. Life Evol. Biosph*. **41**, 469–482.
Boyd, S.A. & Mortland, M.M. (1986). *Environ. Sci. Technol*. **20**, 1056–1058.
Burns, R.G., Burns, V.M. & Stockman, H.W. (1985). *Am. Mineral*. **70**, 205–208.
Chien-To, H. & Hsisheng, T. (2000). *Carbon* **38**, 863–869.
Chitrakar, R., Tezuka, S., Sonoda, A., Sakane, K., Ooi, K. & Hirotsu, T. (2006) *J. Colloid Interface Sci*. **298**, 602–608.
Daou, T.J., Begin-Colin, S. & Greneche, J.M. (2007). *Chem. Mater*. **19**, 4494–4505.
De Guzman, R.N., Shen, Y.F., Shaw, B.R., Suib, S.L. & O'young, C.L. (1993). *Chem. Mater*. **5**, 1395–1400.
Ertem, G. & Ferris, J.P. (1997). *J. Am. Chem. Soc*. **119**, 7197–7201.
Friedmann, N. & Miller, S.L. (1969). *Science* **166**, 766–767.
Ferris, J.P. & Hagan, W.J. (1986). *J. Orig. Life* **17**, 69–84.
Ferris, J.P. & Kamaluddin (1979). *Orig. Life Evol. Biosph*. **19**, 609–619.
Furukawa, T. & Brindley, G.W. (1973). *Clays Clay Miner*. **21**, 279–288.
Graf, G. & Laganly, G. (1980). *Clays Clay Miner*. **28**, 12–18.
Govindraj, N., Mortland, M.M. & Boyd, S.A. (1987). *Environ. Sci. Technol*. **21**, 1119–1123.
Greenland, D.J., Laby, R. & Quirk, J.P. (1962). *Trans. Faraday Soc*. **58**, 829–841.
Greenland, D.J., Laby, R. & Quirk, J.P. (1965). *Trans. Faraday Soc*. **61**, 2024–2035.
Hroacki, S. & Hiromichi, W. (1999). *J. Org. Chem*. **64**, 5836–5840.
Issacson, P.J. & Sawhney, B.L. (1983). *Clay Miner*. **18**, 253–265.
Jortner, J. (2006). *Phil. Trans. R. Soc. B* **361**, 1877–1891.
Julian, C.B. & Suzanne, D.G. (1992). *Clays Clay Miner*. **40**, 273–279.
Kamaluddin (2001). Studies on metal ferrocyanides as prebiotic catalyst. In *First Steps in the Origin of Life in the Universe*, ed. Chela-Flores, J. *et al*., pp. 95. Kluwer Academic Publishers, Netherlands.
Kowalska, M. & Cocke, D.L. (1992). *Clays Clay Miner*. **40**, 237–239.
Kowalska, M.W., Ortego, J.D. & Jezierski, A. (2001). *Appl. Clay Sci*. **18**, 233–243.
Kobayashi, K. & Ponnamperuma, C. (1985a). *Orig. Life* **15**, 55.
Kobayashi, K. & Ponnamperuma, C. (1985b). *Orig. Life* **16**, 67.
Laha, S. & Luthy, R.G. (1990). *Environ. Sci. Technol.*, **24**, 363–373.
Li, L. & Stanforth, R. (2000). *J. Colloid Interface Sci*. **230**, 12–21.
Miller, S.L. (1953). *Science* **117**, 528–529.
Oparin, A.I. (1938). *The Origin of Life*. Macmillan, New York.
Pizzigallo, M.D.R., Ruggiero, P., Crecchio, C. & Mascolo, G. (1998). *J. Agric. Food Chem*. **46**, 2049–2054.
Soma, Y. & Soma, M. (1989). *Chemosphere* **18**, 1895–1902.
Shanker, U., Bhushan, B., Bhattacharjee, G. & Kamaluddin (2011). *Astrobiology* **11**, 225–233.
Shanker, U., Singh, G. & Kamaluddin (2013). *Orig. Life Evol. Biosph*. **43**, 207–220.
Shen, Y.F., Zerger, R.P., Suib McCurdy, L., Potter, D.I. & O'Young, C.L. (1992). *J.* Chem. Chem. Commun. **17**, 1213–1214.
Urey, H. (1952). On the early chemical history of the Earth and the origin of life. *Proc. Natl. Acad. Sci. USA* **38**, 351–363.
Viladkar, S., Alam, T. & Kamaluddin (1994). *J. Inorg. Biochem*. **53**, 69–78.
Visscher, J. & Schwartz, A.W. (1989). *J. Mol. Evol*. **29**, 284–287.
Yao, W. & Millero, F.J. (1996). *Environ. Sci. Technol*. **30**, 536–541.